Mathematical Modeling of Bone Formation and Resorption: Effects of Parathyroid Hormone and Prolactin

Chontita Rattanakul

***Abstract*—**We propose a mathematical model to describe the mechanism of bone formation and resorption based on the effects of parathyroid hormone and prolactin. The singular perturbation technique is then applied to analyze our model. We derived the explicit conditions on the system parameters which detect limit cycle behavior which mimics the oscillatory behavior observed in the clinical data. Finally, numerical investigation is carried out to support our theoretical analysis.

***Keywords*—**bone resorption, parathyroid hormone, prolactin, mathematical model.

I. Introduction

OSTEOPOROSIS represents a major health disorder of bone remodeling in developed countries, affecting over 15 million patients in the United States and costing $ 1 billion per year in medical costs [1]. It is a bone disease where bone mass decreases over time resulting from a net increase of bone resorption over bone deposition. Prevention and reversal of bone loss require a thorough understanding of bone remodeling process, the mechanism of bone formation, and resorption, including the action of hormones such as parathyroid hormone (PTH) and prolactin (PRL).

In bone remodeling, osteoclasts and osteoblasts differentiate from less mature precursors, which line bone surfaces in an inactive state [2]. Bone remodeling can be viewed as a step by step process as follows: osteoclasts appear on a previously inactive surface of bone and then, they excavate a lacuna on the surface of cancellous bone or resorption tunnel in cortical bone. Osteoclasts are subsequently replaced by osteoblasts and finally, osteoblasts refill the resorption cavity [3]. After osteoblasts have laid down their protein-based matrix, known as osteoid, they bury themselves in bony matrix, becoming osteocytes, or revert to an inactive cell form and line the bone surfaces as surface osteocytes or resting osteoblasts [4]. Thus, the number of osteoblasts determines the rate of bone deposition while the number of osteoclasts determines the rate of bone resorption, the balance between the number and activity of osteoblasts and of osteoclasts determines whether net bone deposition or net bone resorption occurs [5]. Bone imbalance can result if the osteoclasts produce an excessively deep resorption space, if the osteoblasts fail to completely refill the resorption space, or if both even occur. If a remodeling imbalance exists after the completion of a remodeling cycle, the degree of bone loss will be exacerbated and that leads to osteoporosis [3].

Bone, being a major reservoir of body calcium, is under the hormonal control, principally of parathyroid hormone (PTH) [2]. The overall effect of PTH is to raise plasma levels of calcium, partly through bone resorption, by the activation of osteoclasts. Osteoclasts resorb bone and liberate calcium but they lack PTH receptors while preosteoblast precursors and preosteoblasts possess them. Therefore, PTH will increase the number of osteoclasts only after having increased the osteoblastic population [5].

PTH is directly controlled by the level of calcium in blood. The decrease of calcium level in blood results in an increase in the secretion of PTH from the parathyroid grand. PTH inhibits the differentiation of preosteoblasts to form osteoblasts [6], [7]. Moreover, PTH stimulates osteoblasts to produce interleukine-6 (IL-6) and in turn, IL-6 stimulates the activity and differentiation of osteoclasts resulting in increased bone resorption [8]. On the other hand, osteoblasts and stromal cells express an osteoclast differentiation factor (ODF) and osteoclasts precursors possess RANK, a receptor of the TNF (tumor necrosis factor) family, which recognizes ODF through the cell-to-cell interaction with osteoblasts [9], [10]. In addition, the binding of ODF by RANK in the presence of macrophage colony-stimulating factor causes preosteoclasts to differentiate into osteoclasts and pre-existing osteoclasts to become activated which also resulted in increased bone resorption and then the level of calcium in blood will be increased [11].

PRL is a polypeptide hormone that is synthesized and secreted from the lactotroph cells in the anterior pituitary gland. Aside from its action on reproduction and lactation, PRL plays a role in maintaining the constancy of the internal environment by regulation of the immune system, osmotic balance and angiogenesis [12]. Moreover, PRL-receptors have been found on the receptors of the osteoblastic cells [13] which are the cells that play a crucial role in the bone

Manuscript received April 9, 2010. This work was supported by the Centre of Excellence in Mathematics, PERDO, Commission on Higher Education, Thailand.

C. Rattanakul is with the Department of Mathematics, Faculty of Science, Mahidol University, Bangkok, Thailand 10400 and the Centre of Excellence in Mathematics, PERDO, Commission on Higher Education, Thailand. (corresponding author, phone: 662-201-5340; fax: 662-201-5343; e-mail: sccrt@mahidol.ac.th).

remodeling process. Hence, PRL can have significant effects on the bone remodeling process as well. It has been found that PRL enhances bone resorption in part by increasing RANKL and decreasing OPG expressions by osteoblasts [14].

There are several attempts such as [5], [15]-[18] to describe bone remodeling process mathematically, however the effect of PRL on the process did not take into account.

Thus, a better understanding of the roles of PTH and PRL in the mechanism of bone remodeling process is crucial to the study of how these secretion systems of physiological importance may be monitored and controlled or regulated for effective preventive therapy measures.

II. MODEL DEVELOPMENT

We now develop a mathematical model of bone formation and resorption based on the effects of PTH and PRL as follows where $T(t)$, $P(t)$, $C(t)$ and $B(t)$ denote the level of PTH above the basal level, the level of PRL above the basal level, the number of activated osteoclasts and the number of activated osteoblasts, respectively.

Firstly, osteoclasts resorb bone and liberate calcium, in order to counter balance the high level of calcium in blood the rate of PTH secretion will decrease [19]. Moreover, the increase of the level of PRL results in the increase of the level of PTH [20]. Therefore, the equation for the rate of PTH secretion is then assumed to take the form

$$\frac{dT}{dt} = \frac{c_1}{k_1 + C} + c_2 P - e_1 T \tag{1}$$

where c_1, c_2, k_1 and e_1 are positive constants.

Secondly, PRL secretion is controlled by the negative feedback of the anterior pituitary gland, when the level of PRL rises to the high level the secretion of PRL will be decreased [12]. Moreover, PTH inhibits the uptake and release of dopamine which is PRL inhibiting factor and hence increases the level of PRL [19]. Therefore, the equation for the rate of PRL secretion is then assumed to take the form

$$\frac{dP}{dt} = \left(c_3 - c_4 P\right) P + c_5 TP - e_2 P \tag{2}$$

where c_3, c_4, c_5 and e_2 are positive constants.

The dynamics of the osteoclastic population can be described by the following equation

$$\frac{dC}{dt} = \left(\frac{\left(c_6 + c_7 T\right)}{k_2 + T^2} + c_8 P \right) BC - e_3 C \tag{3}$$

where the first term on the right-hand side represents the reproduction of active osteoclasts which requires the production of osteoclast differentiation factor (ODF) and its receptor on osteoclasts [5]. The more C means the more ODF receptors available for the reproduction of active osteoclasts, and hence the term is taken to depend on the number of osteoclasts C at that moment in time.

Moreover, osteoclasts precursors possess RANK, a receptor of TNF (tumor necrosis factor) family that recognizes ODF through a cell-to-cell interaction with osteoblasts [9]-[11], hence the rate of reproduction is taken to depend also on the number of active osteoblastic cells $B(t)$ at any time t. However, the rate of reproduction of C increases with the increase in the level of PTH [8], [21]. On the other hand, it has been clinically observed [5] that as PTH level increases further, it begins to inhibit osteoclastic reproduction, and hence the saturation expression $\frac{\left(c_6 + c_7 T\right)}{k_2 + T^2}$ is assumed for the stimulating effect of PTH. In addition, it has been found that PRL enhances bone resorption in part by increasing RANKL and decreasing OPG expressions by osteoblasts [14]. Hence, the increase in the level of PRL results in the increase of the activated osteoclasts and therefore the term $c_8 P$ is also taken in to account where c_6, c_7, c_8, e_3 and k_2 are positive constants.

Finally, the dynamics of the active osteoblastic population B(t) can be described by the following equation

$$\frac{dB}{dt} = c_9 T - \frac{c_{10} TB}{k_3 + T} - e_4 B \tag{4}$$

where c_9 is the specific rate at which PTH stimulates reproduction of active osteoblasts [2],[7]. The second term on the right-hand side of (4) accounts for the inhibiting effect of PTH on osteoblastic differentiation through the process of down-regulation of the PTH receptors on osteoblasts [5] where c_9, c_{10}, k_3 and e_4 are positive constants.

The last terms in the above four equations are the removal rates of the four components of the remodeling process with rate constants e_1, e_2, e_3 and e_4, respectively.

Our model therefore consists of (1)-(4), possessing highly diversified nonlinear characteristics, upon which further analysis and investigation may be carried out in an attempt to explain the mystifying empirical observations previously mentioned.

III. SINGULAR PERTURBATION ANALYSIS

To analyze the nonlinear mathematical model (1)-(4) by the singular perturbation method, we scale the dynamics of the four components of the system by means of two small dimensionless positive parameters ε, δ and η, as follows. Letting $x = T,\ y = P,\ z = C,\ w = B,\ a_1 = c_1,\ a_2 = c_2,\ a_3 = \frac{c_3}{\varepsilon}$, $a_4 = \frac{c_4}{\varepsilon}, a_5 = \frac{c_5}{\varepsilon}, a_6 = \frac{c_6}{\varepsilon\delta}, a_7 = \frac{c_7}{\varepsilon\delta}, a_8 = \frac{c_8}{\varepsilon\delta}, a_9 = \frac{c_9}{\varepsilon\delta\eta}, a_{10} = \frac{c_{10}}{\varepsilon\delta\eta}$, $d_1 = e_1,\ d_2 = \frac{e_2}{\varepsilon},\ d_3 = \frac{e_3}{\varepsilon\delta}$ and $d_4 = \frac{e_4}{\varepsilon\delta\eta}$, we are led to the following system of differential equations.

$$\frac{dx}{dt} = \frac{a_1}{k_1 + z} + a_2 y - d_1 x \equiv f\left(x, y, z, w\right) \tag{5}$$

$$\frac{dy}{dt} = \left(a_3 - a_4 y\right) y + a_5 xy - d_2 y \equiv \varepsilon g\left(x, y, z, w\right) \tag{6}$$

$$\frac{dz}{dt} = \left(\frac{\left(a_6 + a_7 x\right)}{k_2 + x^2} + a_8 y \right) zw - d_3 z \equiv \varepsilon\delta h\left(x, y, z, w\right) \tag{7}$$

$$\frac{dw}{dt} = a_9 x - \frac{a_{10} xw}{k_3 + x} - d_4 w \equiv \varepsilon\delta\eta k\left(x, y, z, w\right) \tag{8}$$

This means that, if ε, δ and η are small, the dynamics of PTH, PRL, activated osteoblasts and activated osteoclasts are assumed to be fastest, intermediate, slow and slowest, respectively. The system of (5)-(8) can be analyzed by applying the singular perturbation technique in the following manner [22] which are based on simple geometric characteristics of the equilibrium manifolds, allowing one to derive conditions that ensure the existence of a limit cycle.

The shapes and relative positions of the manifolds $\{f=0\}$, $\{g=0\}$, $\{h=0\}$ and $\{k=0\}$ determine the directions, speeds, and shapes of the resulting solution trajectories. Therefore, we shall analyze each of the equilibrium manifolds in detail. The delineating conditions for the existence of limit cycle are arrived at from the close inspection of these manifolds.

The manifold { f = 0 }

This manifold is given by the equation

$$y = \frac{1}{a_2}\left(d_1 x - \frac{a_1}{k_1 + z}\right) \equiv U(x,z) \tag{9}$$

We see that this manifold is independent of *w*. It intersects the $(x,z)-$plane along the curve

$$x = \frac{a_1}{d_1(k_1+z)}$$

which intersects the *x*-axis at the point where $z=0$ and

$$x = \frac{a_1}{d_1 k_1} \equiv x_1 \tag{10}$$

Moreover, $U(x,z)$ is an increasing function of x and z.

The manifold { g = 0 }

This manifold consists of two sub-manifolds. One is the trivial manifold $y=0$ while the other one is the nontrivial manifold

$$y = \frac{1}{a_4}\left(a_5 x + (a_3 - d_2)\right) \equiv V(x) \tag{11}$$

which is independent of *z* and *w*. $V(x)$ is an increasing function of x, it intersects the *x*-axis at the point where $y=0$ and

$$x = \frac{1}{a_5}(d_2 - a_3) \equiv x_2 \tag{12}$$

The manifold { h = 0 }

This manifold consists of two sub-manifolds. One is the trivial manifold $z=0$ while the other one is the nontrivial manifold

$$y = \frac{1}{a_8}\left(\frac{d_3}{w} - \frac{a_6 + a_7 x}{k_2 + x^2}\right) \equiv W(x,w) \tag{13}$$

which is independent of *z*. For a fixed value of *w*, the nontrivial manifold $y = W(x,w)$ intersects the *y*-axis at the point where $x=0$ and

$$y = \frac{1}{a_8}\left(\frac{d_3}{w} - \frac{a_6}{k_2}\right) \equiv y_1(w) \tag{14}$$

It attains its minimum at the point where

$$x = \frac{-a_6 + \sqrt{a_6^{\,2} + a_7 k_2}}{a_7} \equiv x_3 \tag{15}$$

and

$$y = \frac{1}{a_8}\left(\frac{d_3}{w} - \frac{a_6 + a_7 x_3}{k_2 + x_3^2}\right) \equiv y_3(w) \tag{16}$$

Moreover, $y \to \frac{d_3}{a_8 w} \equiv y_2(w)$ as $x \to \infty$ and $W(x,w)$ is a decreasing function of w.

The manifold { k = 0 }

This manifold is given by the equation

$$w = \frac{a_9 x^2 + a_9 k_3 x}{(a_{10} + d_4)x + d_4 k_3} \equiv \Psi(x) \tag{17}$$

This manifold is independent of y and z. It intersects the *x*-axis at the point where $w=0$ and $x=0$ or $x=-k_3$, while it intersects the *w*-axis at the point where $x=0$ and $w=0$. Moreover, $\Psi(x)$ is an increasing function of x in the first octant and $w \to \infty$ as $x \to \infty$.

Theorem 1 If ε, δ and η are sufficiently small, and

$$0 < x_2 < x_3 < x_1 \tag{18}$$

$$0 < y_3(w) < y_1(w) \tag{19}$$

where all parametric values are defined as above, then a limit cycle exists for the system of (5)-(8).

The proof of the theorem is based on a geometric singular perturbation method, which were elaborated by [23] and [24] and utilized successfully in many applications [25]-[26]. Under the conditions identified in the theorem, the shapes and relative positions are as in Fig. 1. where the fast parts are indicated by three arrows, the intermediate parts by two arrows, and the slow parts by a single arrow.

In Fig. 1, starting from a generic point A in front of the manifold $\{f=0\}$ and above the manifold $\{h=0\}$, the solution trajectory develops at constant *y* and *z* in the direction of decreasing x since $f<0$ here, and reaches a point B on the fast manifold $\{f=0\}$ at high speed. Then, a transition develops at intermediate speed along manifold $\{f=0\}$ in the direction of decreasing y, since $g<0$ here, towards the point C on the stable branch of the curve $\{f=h=0\}$. A transition develops along this curve at intermediate speed in the downward direction, since $g<0$ here, until it reaches some point D, where the stability of the manifold is lost followed by

a jump to the point E on the other stable branch of the curve $\{f = h = 0\}$ with a fast speed in the direction of increasing x. Here, $g > 0$ and thus a transition will develop at intermediate speed from the point E in the direction of increasing y to the point F where the stability of the manifold is lost followed by a jump to the point G on the other stable branch of the curve $\{f = h = 0\}$ with a fast speed in the direction of decreasing x. A transition develops along this curve at intermediate speed in the downward direction, since $g < 0$ here, until it reaches some point D resulting in a closed cycle DEFG. Therefore, a limit cycle has been identified for the system of (5)-(8).

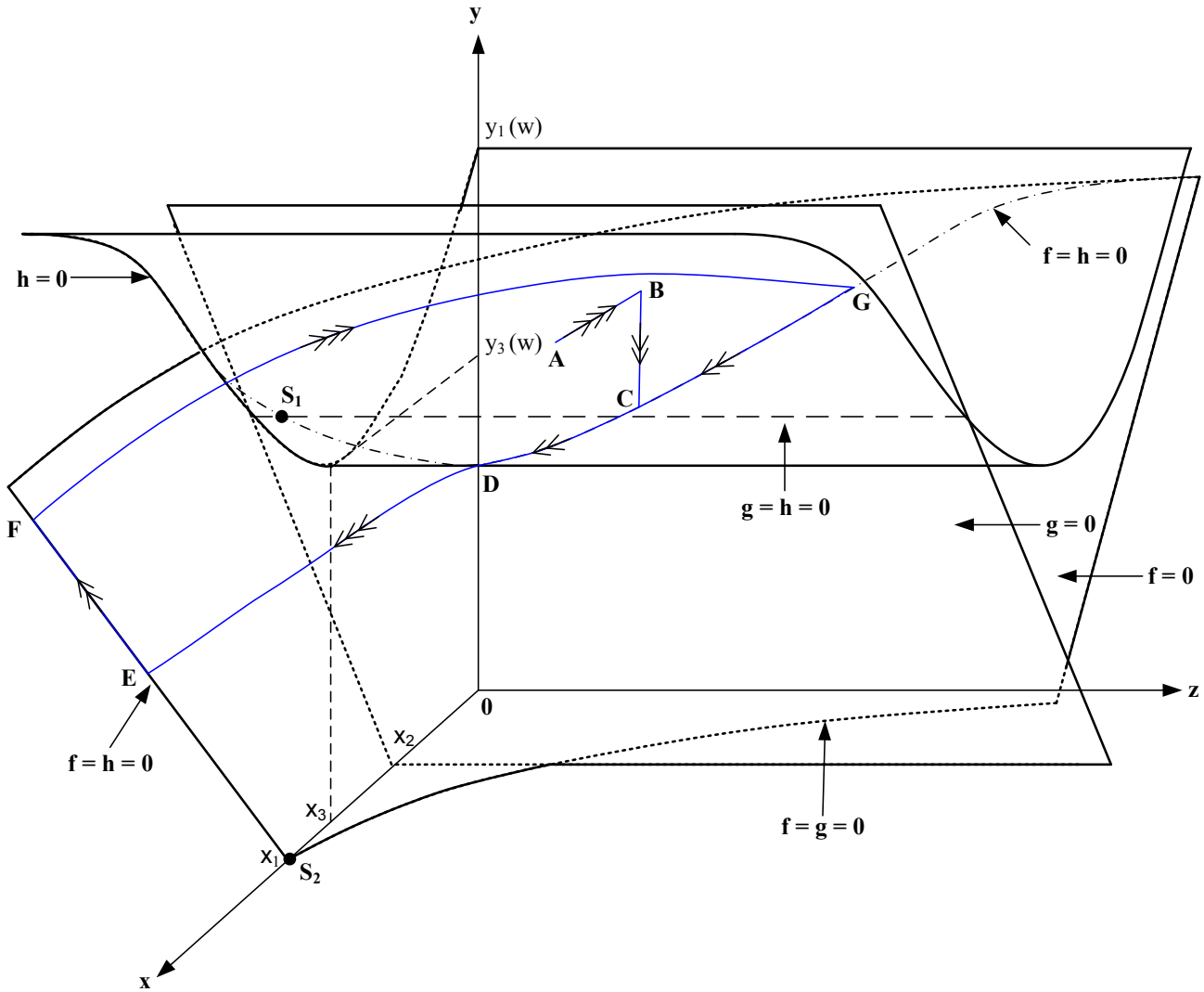

Fig. 1 The three equilibrium manifolds $\{f = 0\}, \{g = 0\}$ and $\{h = 0\}$ in the $(x, y, z)-$space for a particular value of w. and a solution trajectory of the system of (5)-(8) for which the attractor is a limit cycle where all conditions in theorem 1 are satisfied.

IV. NUMERICAL INVESTIGATION

A computer simulation of (5)-(8) is presented in Fig. 2, with parametric values chosen to satisfy the inequalities identified in theorem 1. The solution trajectory, shown in Fig. 2 projected onto the (x,y)-plane, (x,z)-plane, (y,z)-plane and (x,w)-plane tends to a limit cycle as theoretically predicted. The corresponding time courses of PTH, PRL, activated osteoclasts and actived osteoblasts are shown in Fig. 3. Such oscillatory behavior in the level of PTH and PRL has often been observed in clinical data [27]-[29].

V. CONCLUSION

We have demonstrated, through the development and analysis of a model for bone formation and resorption based on the effects of PTH and PRL that the nonlinear dynamic

behavior can be deduced which closely resembles clinical data, even though the model is kept relatively simple.

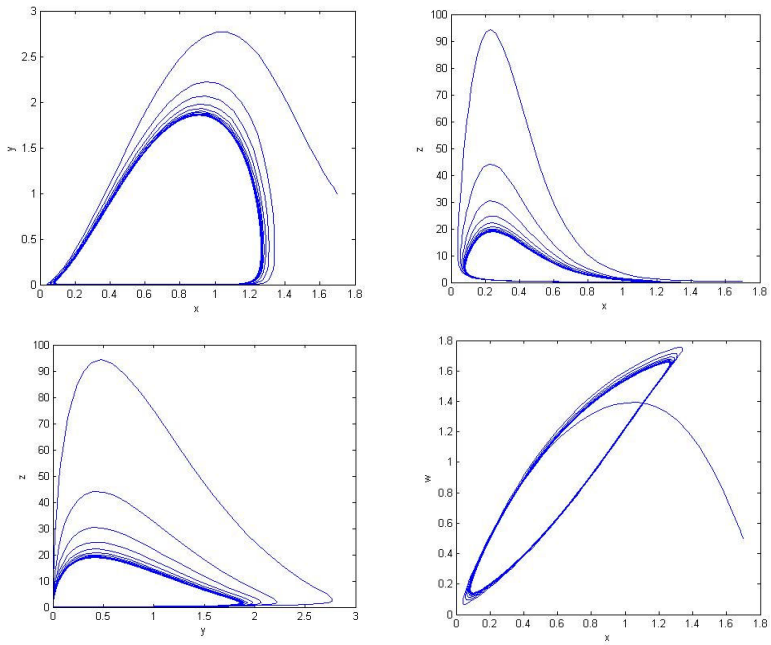

Fig. 2 A computer simulation of the model system (5)-(8) with $a_1 = 0.1, a_2 = 0.01, a_3 = 0.05, a_4 = 0.1, a_5 = 0.7, a_6 = 0.2, a_7 = 0.1,$ $a_8 = 0.25, a_9 = 0.7, a_{10} = 0.1, k_1 = 0.3, k_2 = 0.5, k_3 = 3.2, d_1 = 0.2, d_2 = 0.5, d_3 = 0.3, d_4 = 0.5, \varepsilon = 0.85,$ $\delta = 0.97$ and $\eta = 0.75$ where $x(0) = 1.7, y(0) = 1, z(0) = 0.5,$ $w(0) = 0.5$. The solution trajectory projected onto the (*x,y*)-plane, (*x,z*)-plane, (*y,z*)-plane and (*x,w*)-plane tends to a limit cycle.

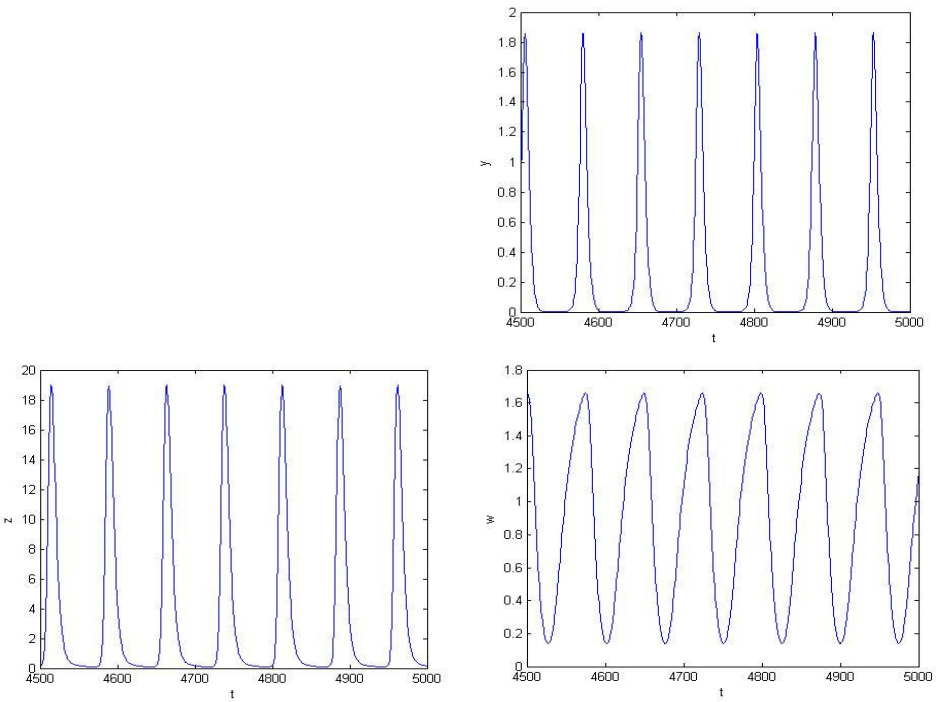

Fig. 3 A computer simulation of the model system (5)-(8) with $a_1 = 0.1, a_2 = 0.01, a_3 = 0.05, a_4 = 0.1, a_5 = 0.7, a_6 = 0.2, a_7 = 0.1,$ $a_8 = 0.25, a_9 = 0.7, a_{10} = 0.1, k_1 = 0.3, k_2 = 0.5, k_3 = 3.2, d_1 = 0.2, d_2 = 0.5, d_3 = 0.3, d_4 = 0.5, \varepsilon = 0.85,$ $\delta = 0.97$ and $\eta = 0.75$ where $x(0) = 1.7, y(0) = 1, z(0) = 0.5,$ $w(0) = 0.5$. The corresponding time courses of PTH, PRL, activated osteoclasts and activated osteoblasts.

REFERENCES

[1] Rosenberg," A Skeletal system and soft tissue tumors", in Robbins Pathologic Basis of Disease, 5th edn, R. S. Cotran, V. Kumar and S. L. Robbins(Eds), Philadelphia:W. B. Saunders Co.,1994, pp.1219-1222.

[2] Brown, E.M., "Extracellular Ca2+ sensing, regulation of parathyroid cell function, and role of Ca2+ and other ions as extracellular (first) messengers", Physiol. Rev., Vol. 71,pp. 371-411.

[3] Russell, T. Turner, B. Lawrence, R. and Thomas, C. S.," Skeletal effects of estrogen", Endocr. Rev., Vol.15(3), 1994, pp.275-300.

[4] Raisz, L. G. and B. E. Kream.," Regulation of bone formation",New Engl. J. Med.,Vol. 309, 1983, pp.29-35.

[5] Kroll, M. H., "Parathyroid hormone temporal effects on bone formation and resorotion", Bull. Math. Bio., Vol 62, 2000, pp.163-188.

[6] Oniya, J. E., J. Bidwell, J. Herring, J. Hulman and J. M. Hock.," In vivo, human parathyroid hormone fragment (hPTH 1-34) transiently stimulates immediate early response gene expression, but not proliferation, in trabecular bone cells of young rats", Bone, Vol.17, 1995, pp.479-484.

[7] Isogai, Y. T., T. Akatsu, T. Ishizuya, A. Yamaguchi, M. Hori, N. Tokahashi and T. Suda, " Parathyroid hormone regulates osteoblast differentiation positively or negatively depending on differentiation stages", J. Bone Mineral Res., Vol.11, 1996, pp.1384-1393.

[8] Weryha, G. and J. Leclere.," Paracrine regulation of bone remodeling", Horm. Res., Vol. 43, 1995, pp.69-75.

[9] Kong,Y.Y. et al. ,"OPGL is a key regulator of osteoclastogenesis, lymphocyte development and lymph-node organogenesis", Nature, Vol. 397, 1999, pp.315-323.

[10] Takahashi, N., N. Udagawa and T. Suda," A new member of tumor necrosis factor ligand family, ODF/OPGL/TRANCE/RANKL, regulates osteoclast differentiation and function", Biochem. Biophys. Res. Commun, Vol. 256, 1999, pp.449-455.

[11] Burgess, T. L. et al.,"The ligand for osteoprotegerin(OPGL) directly activates mature osteoclasts", J. Cell Biol., Vol. 145, 1999, pp.527-538.

[12] Freeman M.E., Kanyicska B., Lerant A. and Nagy G. Prolactin: Structure, Function, and Regulation of Secretion. Physo. Rev. 80(4) (2000): 1523-1631.

[13] Lacroix P.C., Ormandy C., Lepescheux L., Ammann P., Damotte D., Goffin V., Bouchard B., Amling M., Kelly M.G., Binart N., Baron R., Kelly P.A. Osteoblasts are a new target for prolactin: analysis of bone formation in prolactin receptor knockout mice. Endocrinology, 140(1999): 96-105.

[14] Charoenphandhu, N., Tudpor, K., Thongchote, K., Saengamnart, W., Puntheeranurak, S. and Krishnamara, N. High-calcium diet modulates effects of long-term prolactin exposure on the cortical bone calcium content in ovariectomized rats. Am. J. Physiol. Endocrinol. Metab. 2007; 292: E443-E452

[15] Komarova, S.V. Mathematical model of paracrine interactions between osteoclasts and osteoblasts predicts anabolic action of parathyroid hormone. Endocrinology 2005; 146(8): 3589-3595.

[16] Moroz, A.M., Wimpenny, D.I. Allosteric control model of bone remodelling containing periodical modes. Biophy. Chem. 2007; 127:194-212.

[17] Raposo, J.F., Sobrinho, L.G., Ferreira, H.G. A Minimal mathematical model of calcium homeostasis. J. Clin. Endocrinol. Metab. 2002; 87(9): 4330-4340.

[18] Rattanakul, C., Lenbury, Y., Krishnamara, N. and Wollkind, D.J. Mathematical Modelling of Bone Formation and Resorption Mediated by Parathyroid Hormone: Responses to Estrogen/PTH Therapy. BioSystems, 70(2003): 55-72.

[19] Momsen, G., and Schwarz, P., 1997. A mathematical/physiological model of parathyroid hormone secretion in response to blood-ionized calcium lowering in vivo. Scand J. Clin. Lab. Invest. 57, 381-394.

[20] Harvey, S. and Fraser, R.A. Parathyroid hormone: neural and neuroendocrine perspectives. J. Endocrinol. 139(1993): 353-361.

[21] Dempster, D.W., Cosman, F., Parisisen, M., Shen, V. and Linsay, R., 1993. Anabolic actions of parathyroid hormone on bone. Endocr.Rev. 14, 690-709.

[22] Dumrongpokaphan, T. and Lenbury, Y. The analysis of higher-order cascade systems with separation conditions pivoting on the slow components: application to a model of migration for survival of the species. Mathl. Comp. Mod. 38 (2003) 671-690.

[23] Jones, C. K. R. T. Geometric singular perturbation theory. Dynamical systems, Montecatibi Terme, Lecture Notes in Math. 1609(1994) 44-118.

[24] Kaper, T. J. An introduction to geometric methods and dynamical systems theory for singular perturbation problems. Analyzing multiscale phenomena using singular perturbation methods. Proc. Symposia Appl. Math. 56, J.Cronin and R.E.O'Malley Jr. Ed., 1999, American Mathematical Society.

[25] Muratori, S. and Rinaldi, S., 1992. Low-and high-frequency oscillations in three-dimensional food chain systems. Siam J. Appl. Math. 52, 1688-1706.

[26] Lenbury Y., Ruktamatakul S., Amornsamankul S. Modeling insulin kinetics: responses to a single oral gluclose administration or ambulatory-fed conditions. BioSystems. 59(2001): 15-25.

[27] Prank, K., Harms, H., Brabant, G., and Hesch, R.D., 1995. Nonlinear dynamics in pulsatile scretion of parathyroid hormone in normal human subjects. Chaos 5, 76-81.

[28] Roney D.S.M. On a possible psychophysiology of the yogic chakra system. Yoga Magazine, available online July, 2000 (http://www.yogamag.net/ archives/2000/4july00/chakra2.shtml).

[29] Meylan J., Diagnostic methods in female infertility. Reproductive Health. Eds: A Campana, J.J. Dreifuss, P. Sizonenko, J.D. Vassalli and J. Villar. Ares-Serono Symposia Series Frontiers in Endocrinology, Vol. 2 (1993). Ares Serono Symposia Publications, Rome. (http://www.gfmer.ch/books /Reproductive_ health/Diagnostic methods female infertility.html)